

Carbon fluxes in spring wheat agroecosystems in India

Reddy K Narender¹, Gahlot Shilpa², Baidya Roy Somnath², Sehgal Vinay Kumar³, and Vangala Gayatri²

¹Centre for Atmospheric Sciences, Indian Institute of Technology Delhi

²Centre for Atmospheric Sciences, Indian Institute of Technology Delhi

³INDIAN AGRICULTURAL RESEARCH INSTITUTE

November 16, 2022

Abstract

Carbon fluxes from agroecosystems contribute to the variability in the carbon cycle and atmospheric [CO₂]. In this study, we used the Integrated Science Assessment Model (ISAM) equipped with a spring wheat module to study carbon fluxes and their variability in spring wheat agroecosystems of India. First, ISAM was run in the site-scale mode to simulate the Gross Primary Production (GPP), Total Ecosystem Respiration (TER), and Net Ecosystem Production (NEP) over an experimental spring wheat site in the north India. Comparison with flux-tower observations showed that the spring wheat module in ISAM can match the observed flux patterns better than generic crop models. Next, regional-scale runs were conducted to simulate carbon fluxes across the country for the 1980-2016 period. Results showed that the fluxes vary widely, primarily due to variations in planting dates across regions. Fluxes peak earlier in the eastern and central parts of the country, where the crops are planted earlier. All fluxes show statistically significant increasing trends ($p < .01$) during the study period. The GPP, Net Primary Production (NPP), Autotrophic respiration (Ra), and Heterotrophic Respiration (Rh) increased at 1.272, 0.945, 0.579, 0.328, and 0.366 TgC/yr², respectively. Numerical experiments were conducted to study how natural forcings like changing temperature and [CO₂] and agricultural management practices like nitrogen fertilization and water availability could contribute to the increasing trends. The experiments revealed that increasing [CO₂], nitrogen fertilization, and water added through irrigation contributed to the increase of carbon fluxes, with nitrogen fertilization having the strongest effect.

1 **Carbon fluxes in spring wheat agroecosystems in India**

2 **K. N. Reddy^{1*}, S. Gahlot¹, S. Baidya Roy¹, V. K. Sehgal², and V. Gayatri¹**

3 ¹ Centre for Atmospheric Sciences, Indian Institute of Technology Delhi, New Delhi, India.

4 ² Division of Agricultural Physics, ICAR-Indian Agricultural Research Institute, New Delhi,
5 India.

6 Corresponding author: K Narender Reddy (knreddy@cas.iitd.ac.in)

7 **Key Points:**

- 8 • Carbon fluxes in spring wheat agroecosystems vary widely across India due to divergent
9 climatic conditions and management practices, primarily due to different planting dates.
- 10 • All carbon fluxes showed an increasing trend during the 1980 to 2016 study period.
- 11 • Providing sufficient fertilizers and water through irrigation may be able to counteract the
12 adverse effects of high temperatures on carbon fluxes.

13 **Abstract**

14 Carbon fluxes from agroecosystems contribute to the variability in the carbon cycle and
15 atmospheric [CO₂]. In this study, we used the Integrated Science Assessment Model (ISAM)
16 equipped with a spring wheat module to study carbon fluxes and their variability in spring wheat
17 agroecosystems of India. First, ISAM was run in the site-scale mode to simulate the Gross Primary
18 Production (GPP), Total Ecosystem Respiration (TER), and Net Ecosystem Production (NEP)
19 over an experimental spring wheat site in the north India. Comparison with flux-tower
20 observations showed that the spring wheat module in ISAM can match the observed flux patterns
21 better than generic crop models. Next, regional-scale runs were conducted to simulate carbon
22 fluxes across the country for the 1980-2016 period. Results showed that the fluxes vary widely,
23 primarily due to variations in planting dates across regions. Fluxes peak earlier in the eastern and
24 central parts of the country, where the crops are planted earlier. All fluxes show statistically
25 significant increasing trends ($p < .01$) during the study period. The GPP, Net Primary Production
26 (NPP), Autotrophic respiration (Ra), and Heterotrophic Respiration (Rh) increased at 1.272, 0.945,
27 0.579, 0.328, and 0.366 TgC/yr², respectively. Numerical experiments were conducted to study
28 how natural forcings like changing temperature and [CO₂] and agricultural management practices
29 like nitrogen fertilization and water availability could contribute to the increasing trends. The
30 experiments revealed that increasing [CO₂], nitrogen fertilization, and water added through
31 irrigation contributed to the increase of carbon fluxes, with nitrogen fertilization having the
32 strongest effect.

33 **1 Introduction**

34 Croplands are highly productive ecosystems that interact with the atmosphere by exchanging
35 energy, carbon, and water (Lokupitiya et al., 2016). Croplands take up a large amount of carbon
36 from the atmosphere during their short growing season and contribute to the seasonal-scale
37 variability in atmospheric carbon loading. The increase in the atmosphere's carbon levels has
38 complex impacts on agricultural productivity (Yoshimoto et al., 2005; Saha et al., 2020).
39 Temperature, nitrogen fertilizers, and irrigation are all factors that affect crop development and
40 therefore alter the carbon fluxes from the croplands (Lin et al., 2021). Increased temperature can
41 counteract the beneficial effects of increased carbon in the atmosphere (Sonkar et al., 2019).
42 Better-fertilized soils can react better to higher carbon levels (Lin et al., 2021). Lands with limited

43 water availability result in reduced carbon fluxes (Hatfield and Prueger, 2015; Green et al., 2019).
44 Hence, understanding the variability and drivers of carbon fluxes from agroecosystems can help
45 better understand the interactions between the biosphere and atmosphere.

46 Wheat is one of the most widely farmed cereal crops globally and one of the most important staple
47 foods for approximately 2.5 billion people worldwide (Ramadas et al., 2020). Two cultural types
48 of wheat are grown worldwide: winter wheat and spring wheat. Winter wheat is grown in areas
49 with cold weather across Europe, Australia, Russia, and the USA, where it undergoes vernalization
50 during the winter season. Spring wheat is grown in tropical and sub-tropical regions during winters
51 where the temperatures are warmer. In India, spring wheat is generally sown in October-November
52 and harvested between March and April (Ramadas et al., 2020). Spring wheat is the second-largest
53 crop in India in terms of production and cultivated area after paddy. India is second to China in
54 wheat production, with about 107 Mt in 2020, contributing 13.5% of the global wheat supply
55 (FAOSTAT, 2019). Wheat production in India has been on the rise, increasing by 25% since 2008.
56 The area harvested has risen from 28 Mha in 2008 to 29 Mha in 2019 (FAOSTAT, 2019) making
57 spring wheat the second-largest agroecosystem in the country. However, studies of carbon in
58 spring wheat croplands are limited. An extensive review of the variability of carbon fluxes from
59 terrestrial ecosystems conducted by Baldocchi et al. (2018) lacks studies from Indian subcontinent.
60 Hence, this paper focuses on carbon dynamics and its drivers in spring wheat agroecosystems of
61 India.

62 Although many studies have explored carbon fluxes in various terrestrial ecosystems (Zeng et al.,
63 2020), studies on Indian agroecosystems are limited. Most studies in India estimating carbon fluxes
64 have focused on forest biomes (Jha et al., 2013; Pillai et al., 2019). Jha et al. were the first to
65 discuss carbon and energy fluxes across forest biomes. The authors propose that more flux towers
66 be installed in various vegetation ecosystems to generate a robust carbon flux database (Jha et al.,
67 2013). Pillai et al. (2019) investigated the seasonal variation of NEE in the forest biome using flux
68 tower data and a process-based model (Pillai et al., 2019). The research on forest biomes revealed
69 information about India's forest ecosystems that act as carbon sinks. However, agroecosystems are
70 different from the forest biomes not only because the species composition is different but also
71 because agroecosystems are extensively managed. Human intervention in croplands occur through

72 fertilization, pest control activities, tillering, irrigation, and harvesting. Therefore, it is essential to
73 understand the impact of the human management practices on carbon fluxes in agroecosystems.

74 A few studies have looked at carbon fluxes at the site scale over spring wheat agroecosystems in
75 northern India. These include Patel et al. (2011) for the 2008-2009 growing season, Patel et al.
76 (2021) for the 2014-15 growing season, and Kumar et al. (2021) for the 2013-14 growing season.
77 All studies found the typical U-shaped curve in the NEP at diurnal and seasonal scales. The average
78 growing season NEP was in the 5-6 gC/m²/d¹. Patel et al (2021) also reported a negative correlation
79 of NEP with temperature due to higher respiratory losses at higher temperatures. The site-scale
80 studies can only talk about the intra-annual variation of carbon fluxes. Studying interannual
81 variability in the carbon fluxes is not possible because the flux towers are only operational for one
82 or two years. Furthermore, there are very few flux towers, and they are all concentrated in northern
83 India. Because climate and growing conditions vary considerably across the wheat growing
84 regions, it is impossible to extend these studies to understand carbon fluxes at regional scale.

85 Process-based model are widely used as an alternative to observations for studying carbon
86 dynamics (Sándor et al., 2020). These models explicitly characterize known or hypothesized
87 cause-effect links between physiological processes and driving forces in the environment (Chuine
88 and Régnière, 2017). Process-based crop models, driven by atmospheric and other data as inputs,
89 can simulate production, phenology, carbon and energy fluxes, and the interannual variability in
90 the carbon budget of crops (Revill et al., 2019). The major advantage of using the process-based
91 models is that they can be used to conduct numerical experiments to quantitatively evaluate the
92 explicit effect of input parameters and external drivers on crop growth and fluxes (Jones et al.,
93 2017). There are a couple of studies on carbon fluxes in terrestrial ecosystems of India (Banger et
94 al., 2015; Gahlot et al., 2017) but they do not focus on agroecosystems.

95 This study used the Integrated Science Assessment Model (ISAM), a process-based land surface
96 model with bio-geochemical and bio-geophysical components. ISAM was developed to assess the
97 effect of variations in CO₂ concentration on agroecosystems (Jain and Yang, 2005; Song et al.,
98 2013; Yang et al., 2009). ISAM was used for multiple regional and global-scale multimodel studies
99 like the Global Carbon Budget (Le Quéré et al., 2018), the Trends in Net Land-Atmosphere Carbon
100 Exchange (TRENDY) (Zhao et al., 2016), North American Carbon Program (NCAP) (Huntzinger

101 et al., 2012), Large-scale Biosphere-Atmosphere Experiment in Amazonia Data Model
102 Intercomparison Project (LBA-DMIP) (De Gonçalves et al., 2013), and in comparing with forest
103 FACE site observations (De Kauwe et al., 2013).

104 The broad goal of this study is to study carbon dynamics over spring wheat croplands of India and
105 quantitatively estimate the role of different natural and anthropogenic drivers that govern carbon
106 fluxes. The specific objectives of this paper are (i) to evaluate the capability of the ISAM model
107 equipped with a spring wheat module to simulate carbon fluxes in spring wheat croplands by
108 comparing them against field measurements; (ii) to study the spatiotemporal variation in carbon
109 fluxes over spring wheat croplands of India over approximately four decades; and (iii)
110 quantitatively estimate the effect of external drivers, including natural forcings like changing
111 temperature and [CO₂] and agricultural management practices like nitrogen fertilization and water
112 availability on carbon fluxes from spring wheat croplands of India.

113 To the best of our knowledge, there are no long-term regional-scale studies of carbon dynamics
114 over Indian agroecosystems. As mentioned earlier, management practices can strongly affect crop
115 growth and the interaction of crops with land and atmosphere through exchanges of water, energy,
116 nutrients, and carbon. No studies have explored the impact of these management practices on the
117 carbon fluxes in Indian agroecosystems. The current study would be the first to address these issues
118 and hence play an important role in advancing our understanding of terrestrial carbon dynamics.

119 **2 Methodology**

120 2.1 Modeling Approach

121 Gahlot et al. (2020) had implemented a spring wheat module in ISAM and used it to simulate the
122 phenology and production of spring wheat at the site scale for the spring wheat farm site at the
123 Indian Agriculture Research Institute (IARI), Delhi, and regional scale for entire India. The
124 experimental site at IARI was operational for three growing seasons- 2013-14, 2014-15, and 2015-
125 16. Carbon fluxes were measured only during 2013-14 growing season and phenology data was
126 measured during the latter two seasons. The ISAM was calibrated and validated using phenology
127 observations from the 2014-2015 and 2015-2016 growing seasons (Gahlot et al., 2020). Taking
128 this work forward, we used the same model to estimate the carbon fluxes in the spring wheat
129 croplands of India. The modeling approach used in the study is as follows. First, the ISAM model

130 was run in site-scale mode to simulate the carbon fluxes at the IARI site driven by prescribed
131 management data. The simulations were evaluated against field measurements from the IARI site
132 for the 2013-2014 growing season. Next, ISAM was run in regional-scale mode to simulate carbon
133 fluxes over wheat-growing regions of India spanning from 1901 to 2016. Finally, we conducted
134 numerical experiments to simulate the impacts of environmental drivers and agricultural
135 management practices on carbon fluxes.

136 2.2 Model Description

137 This study used the ISAM in the same configuration as Gahlot et al. (2020) to simulate India's
138 spring wheat phenology and production. For brevity, here we only provide a brief description of
139 the model and its configuration. More details are available in Gahlot et al (2020). ISAM has a
140 module for simulating generic C3 crops driven by external forcings and associated land-
141 atmosphere fluxes of carbon, nitrogen, water, and energy in the croplands (Song et al., 2013). The
142 ISAM_{C3_crop} module has static phenology and prescribed LAI using observations from the
143 Moderate Resolution Imaging Spectroradiometer (MODIS) aboard the Terra and Aqua satellites.
144 The ISAM_{C3_crop} module used static root parametrization with fixed rooting depth and fixed root
145 fraction in each soil layer. Gahlot et al. (2020) developed and implemented ISAM_{dyn_wheat} module
146 that can simulate the phenology and fluxes in spring wheat croplands. ISAM_{dyn_wheat} differs from
147 the static version in three schemes: dynamic phenology, carbon allotment, and vegetation structure
148 growth. ISAM_{dyn_wheat} was equipped with dynamic planting date criteria and heat stress modules
149 to simulate the effects of environmental factors on all aspects of spring wheat phenology. Both
150 modules can be run at the site and regional scales at 0.5° X 0.5° spatial and one-hour temporal
151 resolutions.

152 ISAM simulates the processes through which external drivers can affect crop growth. For example,
153 temperature influences maximum carboxylation rates, which regulates carbon assimilation (Song
154 et al., 2013). The ISAM model can simulate nitrogen dynamics and the interactive effects of
155 carbon-nitrogen cycles caused by climate change or increasing [CO₂] (Yang et al., 2009b).
156 Nitrogen fertilisation through deposition onto the soil serves as a nitrogen input to the ISAM
157 nitrogen cycle (A. Jain et al., 2009). When water and mineral N are scarce, the carbon cycle and
158 its assimilation suffer because of reduced carbon allocation to leaves and stems (Song et al., 2013).

159 Added water through irrigation reduces the water stress on crops in water-limited situations,
160 thereby increasing carbohydrate production.

161 2.3 Site Data

162 Field observations on carbon fluxes are limited in India, and none are available in the public
163 domain. We obtained field observations of carbon fluxes for the 2013-14 spring wheat growing
164 season from the IARI, Delhi, experimental spring wheat farm (Bhatia et al., 2014; Kumar et
165 al.,2021). The farm covering 650 square meters is located at 28°40' N, 77°12' E. The site has an
166 EC flux tower that gave Gross Primary Production (GPP), Total Ecosystem Respiration (TER),
167 and Net Ecosystem Production (NEP). The tower had enough area to ensure an upwind stretch of
168 homogeneous vegetation, which was essential for measuring fluxes using the EC technique
169 (Schmid, 1994). The spring wheat crop was planted on 16 December 2013 at the site. Nitrogen
170 fertilizer at the rate of 120 kg N/ha was applied in three instalments of 60 kg N/ha, 30 kg N/ha,
171 and 30 kg N/ha on the planting day and 25th and 67th days after sowing, respectively. The field
172 was irrigated five times throughout the growing season to avert water stress.

173 2.4 Meteorological and management data

174 All ISAM simulations need data for both environmental and anthropogenic drivers. We used
175 annual atmospheric [CO₂] data from Le Quéré et al. (2018) and climate data from Viovy (2018)
176 for both site scale and country scale simulations. The temporal resolution of the climate data is 6-
177 hourly, and we interpolated the climate data to hourly values. The planting date, nitrogen, and
178 irrigation data used for the site scale runs are described in Section 2.2.

179 For the country scale runs, we used nitrogen fertilizer data developed by Gahlot et al. (2020) by
180 combining data from Ren et al. (2018) and Mueller et al. (2012). Data of harvested wheat area in
181 a gridded format is needed (1980-2016) for calculating fluxes at a country scale in units of TgC/yr.
182 We used spring wheat harvested area data developed by Gahlot et al. (2020), combining harvested
183 area from Monfreda et al. (2008) and MAFW (2017).

184 2.5 Experimental Design

185 2.5.1 Site scale simulations at the IARI site

186 The ISAM model was calibrated and validated by Gahlot et al. (2020) using the phenology
187 observations from the 2014-2015 and 2015-2016 growing seasons. We designed the site
188 scale carbon flux experiment to evaluate the capability of ISAM model to replicate the
189 carbon fluxes from field observations for the growing season 2013-14. To simulate the
190 carbon fluxes at a site scale, the ISAM model was spun up for the 2013-14 growing season
191 using climate data from Viovy (2018), annual atmospheric [CO₂] data from Le Quéré et al.
192 (2018), and airborne nitrogen deposition data (Dentener, 2006) until the soil parameters
193 reached a steady state. Further details on the site scale spin-up are available in Gahlot et al.
194 (2020).

195 We used both variants of the ISAM, the C3 generic crop module (ISAM_{C3_crop}) and the
196 dynamic spring wheat crop module (ISAM_{dyn_wheat}) developed by Gahlot et al. (2020), to
197 simulate crop phenology and carbon fluxes for the 2013-14 growing season. For these
198 simulations, we used the planting date, irrigation, and nitrogen fertilization schedule
199 applied at the IARI site (Section 2.2).

200 2.5.2 Country-wide simulations over wheat-growing regions of India

201 The country-wide simulations were designed to understand the spatial variation of carbon
202 fluxes across India's wheat growing regions by utilising the ISAM_{dyn_wheat} module. To
203 simulate the carbon fluxes at a regional scale, ISAM was spun up for 1901 to maintain
204 constant soil parameters such as temperature, moisture, and carbon and nitrogen pools. For
205 the spin-up, we used the climate data from Viovy (2018) for the years 1901–1920, with
206 airborne nitrogen deposition (Dentener 2006) and [CO₂] (Le Quéré et al., 2018) held at
207 levels of 1901 and neglecting nitrogen fertilizer and irrigation.

208 After a steady-state was observed in the soil parameters, we used ISAM to conduct
209 regional-scale simulations over wheat-growing regions of India to understand the
210 variability of carbon fluxes across diverse climate and management conditions (Ortiz *et al.*
211 2008) from 1901 to 2016. First, we conducted a control run (S_{CON}) driven by the annual
212 [CO₂] data, climate data, nitrogen fertilizer data, and full irrigation to meet crop water

213 needs. Irrigation is a crucial factor in spring wheat cultivation, where 93.6 % of the wheat
214 area is equipped with irrigation (MOA 2016), and the Indo-Gangetic plains contribute a
215 significant part to the total wheat area irrigated in India (Gahlot et al., 2020). Data on the
216 exact volume of irrigation water was not available. Therefore, in the S_{CON} simulation, each
217 grid cell was considered 100% irrigated so that there was no water stress on the crops
218 (Gahlot et al. 2020).

219 Our analysis focused on the years 1980 to 2016. We analyzed country-scale model results
220 as inter-decadal changes from the 1980s to the 2010s. We calculated decadal averages for
221 various fluxes by dividing the total period into 1980s – 1980 to 1989, 1990s – 1990 to
222 1999, 2000s - 2000 to 2009, and 2010s - 2010 to 2016.

223 2.5.3 Experiments to estimate the effect of external drivers on carbon fluxes.

224 Environmental drivers like temperature and $[CO_2]$ and agricultural management practices
225 like applying nitrogen fertilizers and irrigation influence spring wheat growth and are likely
226 to influence carbon fluxes. We conducted four additional experimental simulations to
227 quantitatively estimate the effect of these forcings. The details of the experiments are given
228 in Table 1. In the Control run (S_{CON}), the model was driven by inputs based on observations
229 that vary over time. In the experimental simulations, value of an input driver was kept
230 constant during the study period, while others were allowed to vary as in the S_{CON}
231 simulation. For example, in S_{Temp} , the input data for $[CO_2]$, nitrogen, and irrigation were
232 identical to that in S_{CON} , except for temperature, for which we used the de-trended 1900 –
233 1930 climatology. In the S_{N_Fert} case, the $[CO_2]$, temperature and irrigation were identical
234 to that in S_{CON} , and nitrogen fertilization is absent. The S_{Water} case is like S_{CON} , with the
235 only difference that precipitation climatology was used, and no additional water was
236 provided to the soil through irrigation. We calculated the effect of the individual driver as
237 the difference between the S_{CON} run and the numerical experiments.

238 Table 1

239 *Numerical experiments conducted to evaluate the effect of external drivers on carbon fluxes using*
 240 *ISAM dynamic wheat crop for 1901 – 2016.*

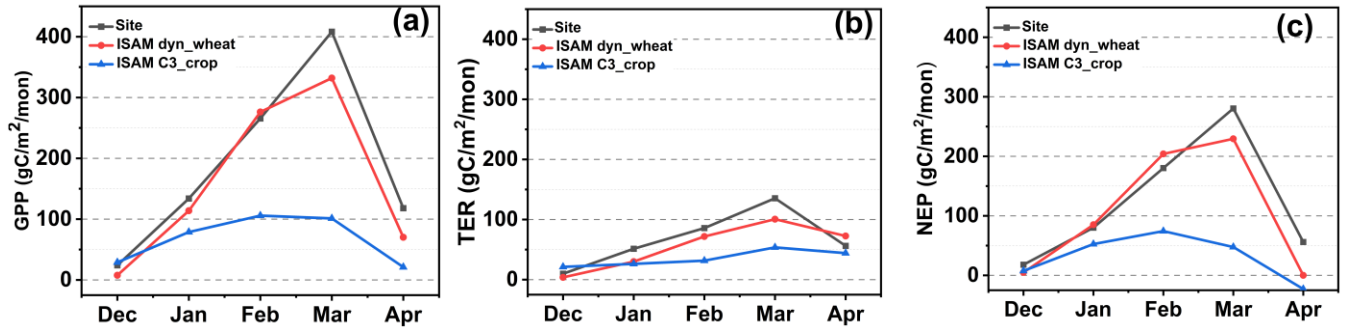
Numerical Experiment	Temperature	[CO₂]	Nitrogen Fertilization	Irrigation
Control (S _{CON})	Six hourly CRU-NCEP	Yearly values from Global Carbon Project Budget 2017	Grid-cell specific fertilizer amount	Hourly values to ensure no water stress
S _{Temp}	Climatological daily temperature prepared from the period 1900-1930	Identical to S _{CON}	Identical to S _{CON}	Identical to S _{CON}
S _{CO2}	Identical to S _{CON}	Fixed at 1901 level	Identical to S _{CON}	Identical to S _{CON}
S _{N_Fert}	Identical to S _{CON}	Identical to S _{CON}	No fertilizer	Identical to S _{CON}
S _{Water}	Identical to S _{CON}	Identical to S _{CON}	Identical to S _{CON}	No irrigation + No precipitation change

241 **3 Results**

242 3.1 Evaluation of ISAM site-scale simulations

243 Site scale simulations were required to evaluate the performance of the dynamic spring wheat
 244 module (ISAM_{dyn_wheat}) implemented in ISAM by Gahlot et al. (2020) in simulating carbon fluxes.
 245 Our results show that the spring wheat module can simulate the magnitude and seasonality of
 246 carbon fluxes in spring wheat croplands better than the generic crop growth module in ISAM
 247 (ISAM_{C3_crop}). Figure 1 and Table 2 compare ISAM_{dyn_wheat} and ISAM_{C3_crop} against site
 248 observations for monthly average fluxes for the 2013-2014 growing season. Figure 1 shows that

249 the observed carbon fluxes started increasing from leaf emergence in mid-December 2013. The
 250 fluxes increased till they reach their peaks in March, after which they declined till the harvest in
 251 April.



252
 253 Figure 1: Comparison of observation and ISAM model fluxes (a) GPP, (b) TER, and (c)
 254 NEP.

255 The simulated fluxes followed the observed pattern. ISAM_{dyn_wheat} model run was in better
 256 agreement with site observations than the ISAM_{C3_crop} model. ISAM_{dyn_wheat} captured the
 257 seasonality and accumulated GPP, TER, and NEP for the growing season better than the
 258 ISAM_{C3_crop} model (Table 2). The ISAM_{dyn_wheat} peak coincided with the observations, whereas
 259 the fluxes simulated by the ISAM_{C3_crop} model peaked about a month earlier. The ISAM_{dyn_wheat}
 260 model in ISAM compares better with site measurements for plant biomass at harvest and maximum
 261 LAI than the ISAM_{C3_crop} model (Table 2).

262 Table 2

263 *Various crop parameters of ISAM_{dyn_wheat} and ISAM_{C3_crop} against site measurements. We*
 264 *compared field observations at the IARI experimental wheat farm site and ISAM crop varieties,*
 265 *the dynamic crop and C3 generic crop, for the growing season of 2013-2014.*

Variable	Site	ISAM _{dyn_wheat}	ISAM _{C3}
Cumulative GPP (gC/m ²)	882	799.90	335.65
Cumulative TER (gC/m ²)	304	278.59	176.63
Cumulative NEP (gC/m ²)	576	523.30	159.02
TER/GPP	0.34	0.35	0.53

Plant Biomass at harvest (t/ha)	13.92	11.71	--
Correlation coefficient TER and GPP	0.86	0.81	0.24
Maximum LAI	4.6	6.0	1.10

266 Table 3 shows the Willmott index and RMSE for the two ISAM runs against the site observations.
 267 The Willmott index is a more sophisticated tool for evaluating the efficiency of land surface
 268 models compared to the usual statistical data comparison indices (Song et al., 2013; Willmott et
 269 al., 2012). The Willmott index (Eq. 1) ranges from -1 to 1, where -1 indicates no agreement while
 270 +1 indicates perfect agreement. The Willmott index for GPP, TER, and NEP for the ISAM_{dyn_wheat}
 271 model are 0.85, 0.73, and 0.83, respectively. The corresponding values for the ISAM_{C3_crop} model
 272 are much lower at 0.47, 0.46, and 0.47, respectively. The higher index value for the dynamic crop
 273 suggested a better agreement of ISAM_{dyn_wheat} over ISAM_{C3_crop} with the site scale observations.
 274 Therefore, the ISAM_{dyn_wheat} model is more appropriate for representing spring wheat dynamics in
 275 the ISAM land model.

$$276 \text{ Willmott index} = \begin{cases} 1 - \frac{\sum_{i=1}^n |Model_i - Obs_i|}{c * \sum_{i=1}^n |Obs_i - \overline{Obs}|}, & \text{if } \sum_{i=1}^n |Model_i - Obs_i| \leq c * \sum_{i=1}^n |Obs_i - \overline{Obs}| \\ \frac{c * \sum_{i=1}^n |Obs_i - \overline{Obs}|}{\sum_{i=1}^n |Model_i - Obs_i|} - 1, & \text{if } \sum_{i=1}^n |Model_i - Obs_i| > c * \sum_{i=1}^n |Obs_i - \overline{Obs}| \end{cases} \quad (1)$$

$$277 \text{ RMSE} = \sqrt{\frac{\sum_{i=1}^n (Model_i - Obs_i)^2}{n}} \quad (2)$$

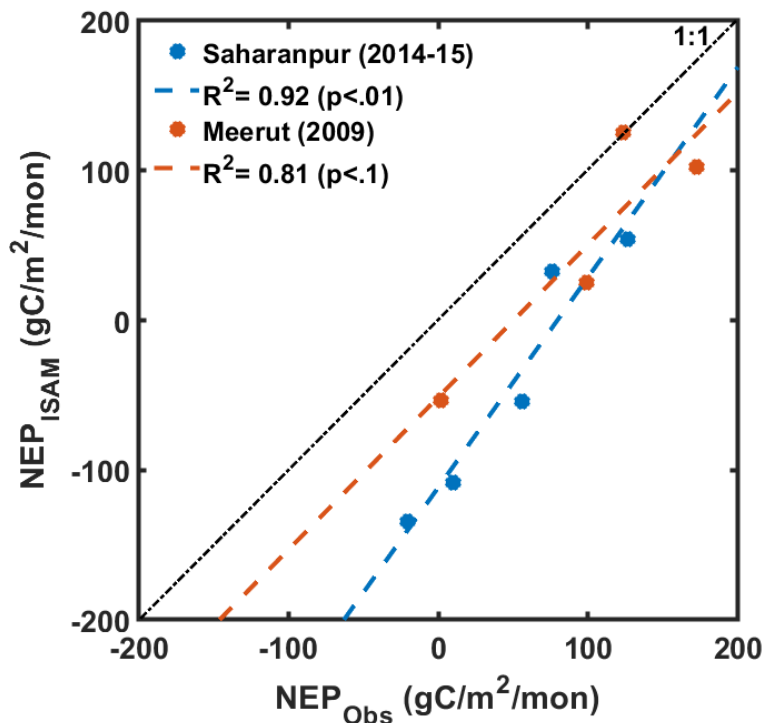
278 where $c = 2$, $n =$ number of observations, $Model_i$ represents the ISAM simulated carbon
 279 fluxes, and Obs_i represents the site scale observations.

280 Table 3

281 *Willmott index and RMSE (gC/m²/mon) of monthly carbon fluxes (GPP, NEP, and TER).*

	Willmott index		RMSE	
	ISAM _{dyn_wheat}	ISAM _{C3_crop}	ISAM _{dyn_wheat}	ISAM _{C3_crop}
GPP	0.85	0.47	42.14	162.62
TER	0.73	0.46	20.82	45.90
NEP	0.83	0.47	36.05	120.44

282 3.2 Spatio-temporal variability of carbon fluxes from spring wheat agro-ecosystems in India

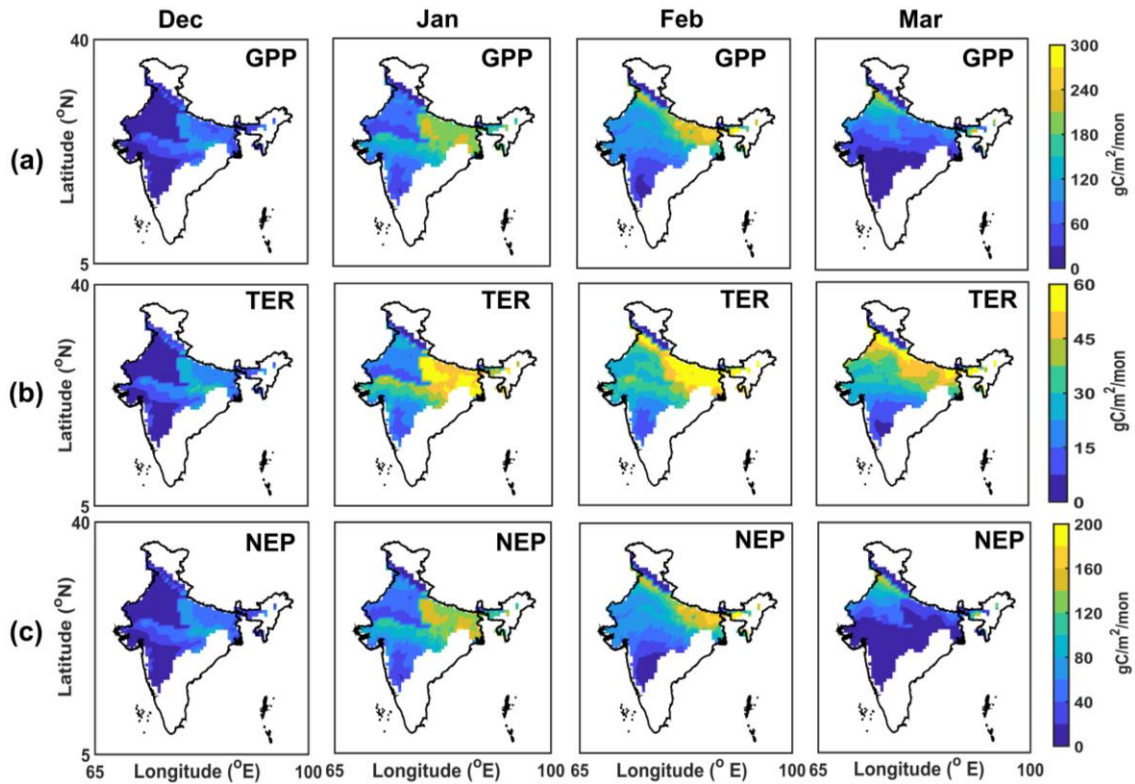


283
 284 Figure 2: Comparison of the ISAM S_{CON} with the observations from Meerut (Patel et al., 2011)
 285 and Saharanpur (Patel et al., 2021).

286 The country-scale S_{CON} run described in Section 2.4b were designed to provide a quantitative
 287 understanding of the spatiotemporal variability of carbon fluxes across the wheat-growing regions
 288 of India. Before evaluating the regional scale ISAM runs, we decided to compare the simulated
 289 NEP from S_{CON} run with the carbon flux data from Patel et al. (2011, 2021). The monthly averaged
 290 carbon flux data was digitized from the figures. Patel et al. (2011) measured the carbon fluxes
 291 from Jan-Apr 2009 over a spring wheat farmland in Meerut in northern India. The measurements
 292 provided a diurnal variation of NEE during four growing stages- tillering, anthesis, post-anthesis,
 293 and at maturity. The diurnal data at a growing stage was averaged, and a value representing a
 294 monthly NEE was calculated and converted to NEP. Patel et al. (2021) provided daily NEE values
 295 at a spring wheat farmland in Saharanpur in northern India. The Patel et al. (2021) data was used
 296 to generate the monthly average fluxes for the growing season 2014-2015. The simulated NEP at
 297 the grid cells where Meerut and Saharanpur are located are extracted from the S_{CON} output. Figure
 298 2 represents the comparison of simulated monthly average NEP (NEP_{ISAM}) and NEP_{OBS} measured

299 at Meerut (2009) and Saharanpur (2014-2015). The R^2 value for the stations is high, showing that
300 the ISAM simulated NEP captures the variation in observed NEP. The significance of the R^2 is
301 calculated using the two-tailed t-test, and the results reveal that R^2 is significant at $p < .01$ at
302 Saharanpur and $p < .1$ at Meerut. The mean absolute bias between observed and simulated NEP at
303 Saharanpur and Meerut are $90.61 \text{ gC/m}^2/\text{mon}$ and $50.227 \text{ gC/m}^2/\text{mon}$, respectively. The bias is
304 perhaps because we are comparing site-scale observations with simulated values that are averaged
305 over the $0.5^\circ \times 0.5^\circ$ ($\sim 2500 \text{ km}^2$) grid cell area. Nonetheless, the high correlations with site
306 observations points to the robustness of the ISAM simulations.

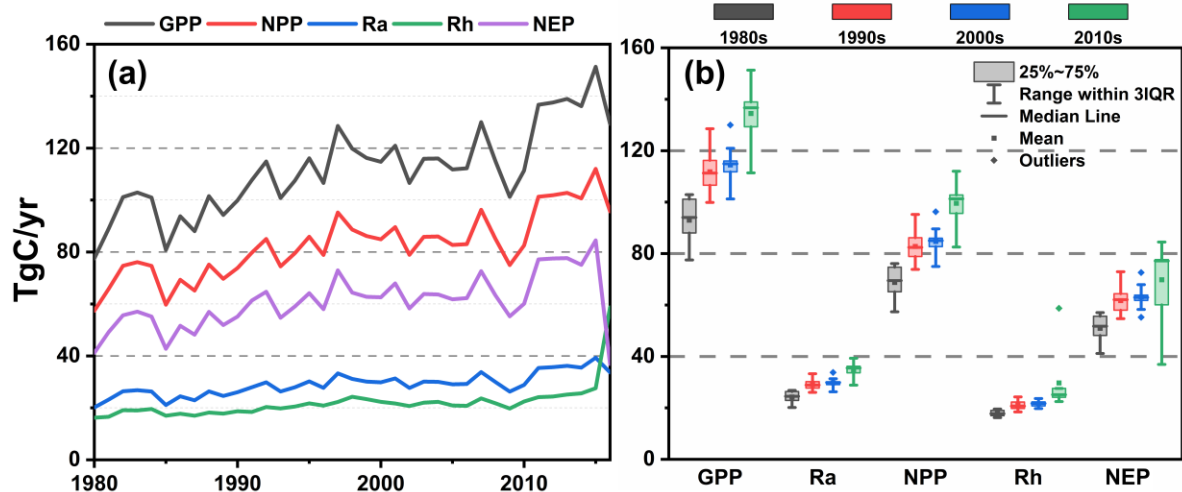
307 Figure 3 shows the spatial maps of GPP, TER, and NEP for the growing season (December to
308 March). The fluxes for each month of the growing season were averaged over sixteen years (2000
309 - 2016) for that specific month. Because the climatic conditions across wheat-growing regions of
310 India are diverse, the wheat crops are sown on different dates, which was reflected in the ISAM
311 model using the dynamic planting day criteria. Spring wheat is planted in late October in Central
312 India and in early November in Eastern India. The planting dates for Northern and North-western
313 regions are late November to early December. Consequently, there are regional variations in the
314 seasonal flux dynamics. The central and eastern parts of the wheat-growing region show the
315 maximum value of fluxes in January and February, respectively, while the northern and western
316 parts show the maxima in March. The spatial plots show very low values of GPP and NEP during
317 December because the crops are still in early growth. The croplands show very low values of NEP
318 during March in the central and eastern parts of wheat-growing regions. Even though the croplands
319 are not active, heterotrophic respiration leads to moderate values of TER in March for the eastern
320 and central parts of India.



321
 322 Figure 3: A spatial variation of (a) GPP, (b) TER, and (c) NEP over the wheat-growing regions of
 323 India averaged over the period 2000 to 2016.

324 Figure 4(a) depicts the temporal pattern of annual and decadal fluxes. From 1980 to 2016, the GPP,
 325 NEP, NPP, Ra, and Rh over the spring wheat croplands increased at 1.272, 0.945, 0.579, 0.328,
 326 and 0.366 TgC/yr², respectively. The trends represent the slope of the linear trend line, and the
 327 trends are significant at $p < .01$ calculated using a two-tailed test. Figure 4(b) shows the box-whisker
 328 plots. The box represents the 25-75 percentile of the data, and the whisker shows three times the
 329 interquartile range (3IQR). The data outside this 3IQR whisker is an extreme outlier. The median
 330 of all the fluxes showed a greater increase from the 1980s to 1990s compared to the 1990s to
 331 2000s. The rise was again steep from the 2000s to the 2010s. Numerical experiments (Table 1)
 332 were conducted to explain the reasons for such behaviour. The results are described in the next
 333 section.

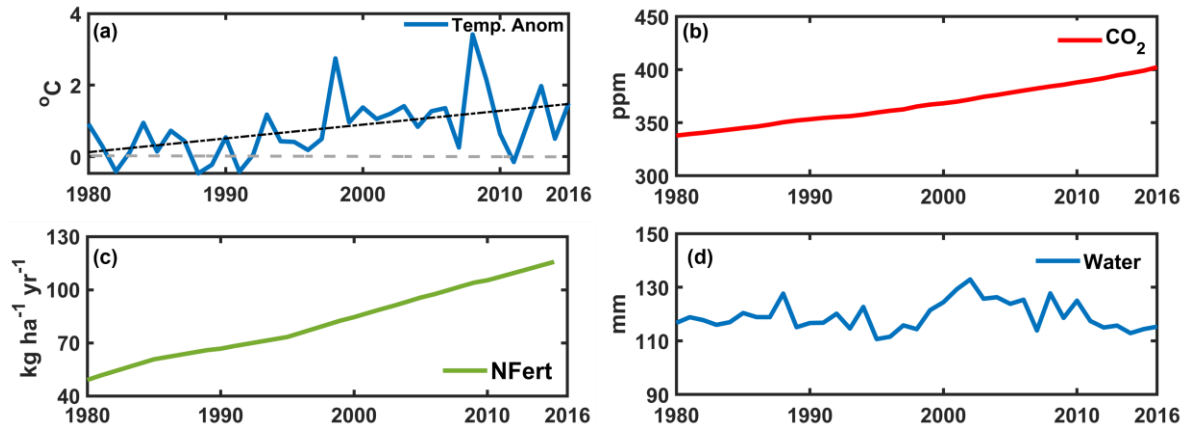
334



335
336 Figure 4: Carbon fluxes simulated by ISAM model. (a) The time series of fluxes from 1980 to
337 2016, (b) Decadal averages of fluxes.

338 3.3 Effects of external drivers on carbon fluxes

339 We investigated the impact of two climate drivers, changing temperature and [CO₂], and two
340 agricultural practices, nitrogen fertilizer and water availability due to irrigation, on carbon fluxes
341 from spring wheat croplands. Figure 5 depicts the variation of these variables. Figure 5(a) shows
342 the temperature anomaly between the S_{CON} and S_{Temp}. The temperatures are always warmer in S_{CON}
343 compared to S_{Temp}. During the study period, the temperature anomaly increased at 0.038 °C/yr
344 (Figure 5:(a)). [CO₂] has also shown a consistent rise and increased at 1.743 ppm/yr (Figure 5:(b)).
345 The nitrogen fertilizer added to the C3 crops increased at 1.86 kg/ha/yr over 36 years from 1980
346 to 2016 (Figure 5:(c)) (Hurt *et al.* 2011). Figure 5(d) displays the anomaly in water present in the
347 root zone during the growing season, estimated as the difference between S_{CON} and S_{Water}.
348 Irrigation increases the amount of water available to crops during the growing season in the S_{CON}
349 run. The S_{CON} run provides ~120 mm/season more water to the crop than the S_{Water} run, which is
350 ~50% of the wheat crop water requirement during the growing season.

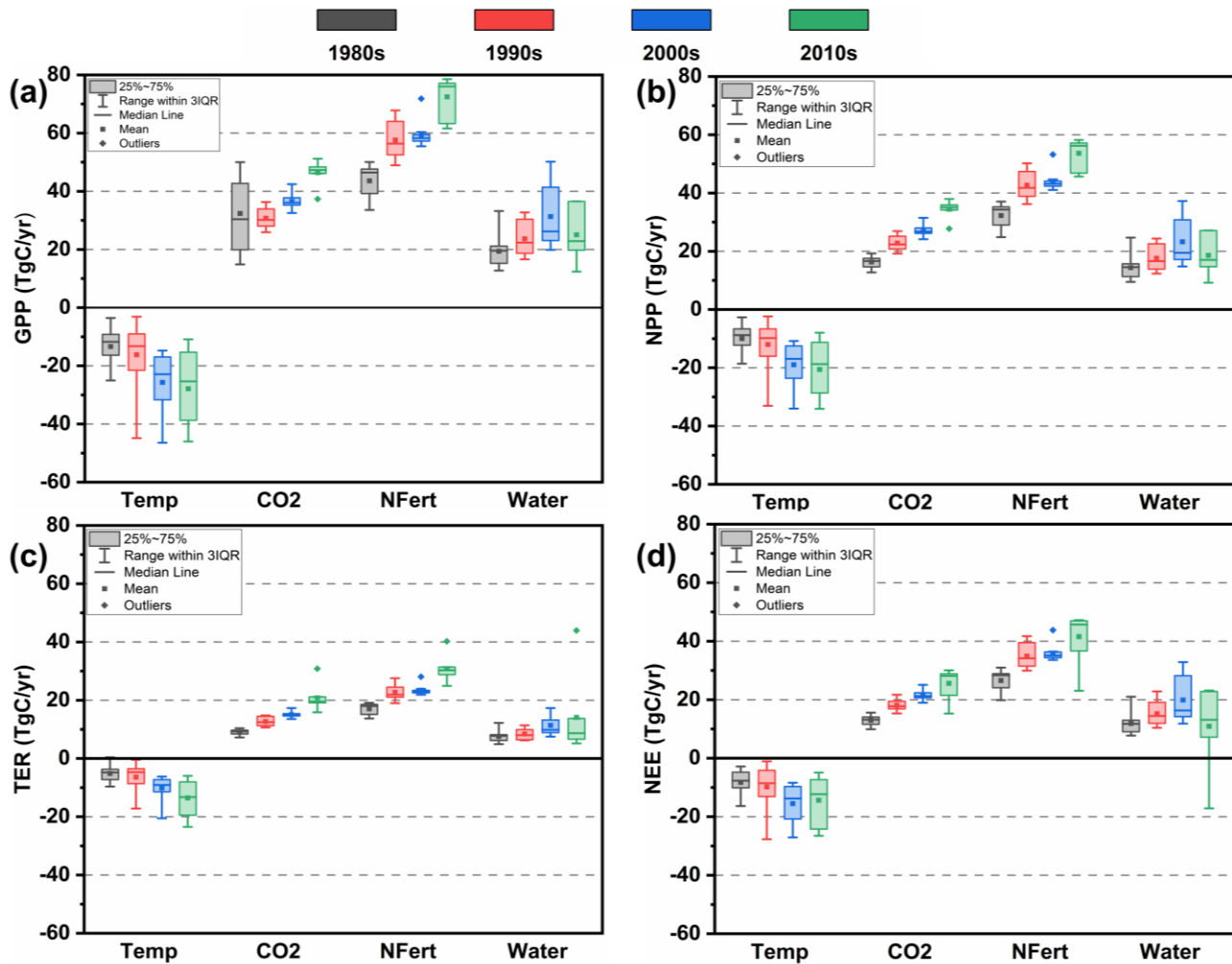


351
 352 Figure 5: Time series of climate variables (a) Temperature anomaly, (b) Carbon Dioxide and
 353 management practice, (c) Nitrogen fertilization, and (d) Anomaly in water available in the root
 354 zone ($S_{CON} - S_{Water}$) during the growing season.

355 The effects of these factors are estimated by analyzing the difference in simulated carbon fluxes
 356 between the control and experimental simulation (Figure 6 and Table 4). Results show that the
 357 increase in temperature has a negative effect on all the fluxes. The temperature anomaly rose at
 358 $0.038\text{ }^{\circ}\text{C}/\text{yr}$, and yearly GPP decreased at $0.597\text{ TgC}/\text{yr}^2$ during the study period. The temperature
 359 has varied less between the 1980s and 1990s; therefore, a slight difference in median GPP between
 360 these two decades is observed (Figure 6: (a)), although a higher spread in GPP is observed in the
 361 1990s which is reflective of a few growing seasons with considerable temperature variation. The
 362 consistent higher temperatures during the 2000s and 2010s have caused a significant decrease in
 363 GPP. Since the temperatures considerably varied during the 2000s and 2010s, a large spread in
 364 simulated GPP can be observed. Similar trends in NPP and NEP can be observed with a decrease
 365 of 21.9 and 13.9 TgC/yr , respectively, per degree rise in temperature. Due to a temperature rise,
 366 the growing period and the crop phenology shortens (Koehler et al., 2013); hence a decrease in
 367 fluxes is observed. As the growth of the crop decreases, the TER and NEP also decreases.

368 Results showed that the increase in $[\text{CO}_2]$ alone has led to a rise in annual GPP, NEP, Ra, and Rh
 369 at 0.805, 0.422, 0.201, and 0.175 TgC/yr^2 , respectively (Table 4). During the study period, $[\text{CO}_2]$
 370 rose at 1.743 ppm/yr, causing an increase in GPP by 462 GgC per year for a unit ppm rise in $[\text{CO}_2]$.
 371 The GPP had a consistent rise each decade. A large spread in GPP was observed in the 1980s. The
 372 $[\text{CO}_2]$ has consistently increased (Figure 5:(b)), but the temperature anomaly in the 1980s was
 373 below zero for a few growing seasons. Therefore, a significant variation in GPP and other fluxes

374 was observed (Figure 4:(a)) in this decade. Similarly, due to a higher CO₂ availability for the wheat
 375 crops, NPP, NEP, and TER have increased by 202, 100, and 173 GgC/yr per ppm rise in [CO₂].
 376 As the [CO₂] level increases in the environment, more carbon is available for crop uptake by
 377 photosynthesis (Saha et al., 2020).



378
 379 Figure 6: The Impact of various drivers (red- natural drivers: CO₂ and temperature, and blue-
 380 agricultural practices: irrigation and nitrogen fertilization) on wheat carbon fluxes. The impact of
 381 CO₂ is $S_{CON} - S_{CO_2}$. Similarly, the impact of temperature is $S_{CON} - S_{Temp}$, nitrogen fertilization is
 382 $S_{CON} - S_{N_Fert}$, and irrigation is $S_{CON} - S_{Water}$.

383 Nitrogen fertilization has led to an increase in NEP, Ra, and Rh at 0.468, 0.231, and 0.197 TgC/yr²,
 384 respectively. The impact of nitrogen fertilization on GPP at 0.897 TgC/yr² was the highest among
 385 all the factors. Nitrogen fertilization caused an increase in GPP by ~33 TgC on an annual basis.

386 Similarly, NEP increased by ~17 TgC/yr, Ra and Rh by ~8 and ~7 TgC/yr, respectively. Nitrogen
 387 fertilization is essential in India due to its tropical climate and multiple cropping systems (Gahlot
 388 et al., 2020). Studies have shown that nitrogen availability impacts the carbon uptake through the
 389 process of progressive Nitrogen limitation (A. Jain et al., 2009). Though the progressive nitrogen
 390 limitation is observed over longer timescales than the growing period of the crops, the decadal
 391 carbon flux simulations revealed some interesting results. Under excess [CO₂] but nitrogen limited
 392 conditions, the crop growth does not show large difference and therefore the carbon uptake
 393 decreases (A. Jain et al., 2009; Luo et al., 2006). Under excess [CO₂], if sufficient nitrogen is
 394 available then the carbon uptake by the ecosystem increases and therefore the maximum increase
 395 in fluxes was observed in the nitrogen fertilization case (Table 4). Nitrogen fertilization was
 396 consistent over the decades leading to a constant rise in GPP, but the variation in GPP in the 2000s
 397 was the least (Figure 6) caused by high temperatures during this decade (Figure 5). A similar
 398 pattern of low variation was observed in NEP, Ra, Rh and NEP during this period.

399 Table 4

400 The impact of each driver (TgC/yr²) on various fluxes of the spring wheat crop in India. The
 401 values show the slope giving the linear trend of individual fluxes. *The trend has a significance
 402 level of $p < .01$.

Driver	GPP	Ra	NPP	Rh	NEP
Temperature	-0.597*	-0.159*	-0.438*	-0.185*	-0.278*
[CO ₂]	0.805*	0.201*	0.597*	0.175*	0.422*
Nitrogen Fertilization	0.897*	0.231*	0.666*	0.197*	0.468*
Water	0.243	0.062	0.182	0.173	0.01

403 The impact of water added through irrigation led to an annual increase of ~9 TgC in GPP, ~6.5
 404 TgC in NPP, ~2 TgC in Ra, and ~6 TgC in Rh. The reason for a small trend was that the fluxes
 405 have increased through the 1980s, 1990s, and 2000s, but declined in the 2010s. The reason for the
 406 decline was less water availability for the crops during this period, as shown in Figure 5(d).
 407 Therefore, the trends in these fluxes are not significant (Table 4). The higher GPP, NPP, and NEE
 408 in the 2000s compared to 1990s even though the temperatures were higher in 2000s suggested that

409 the adverse effects of high temperatures can be overcome if the crops are provided with enough
410 water.

411 **4 Discussions**

412 The ISAM simulations and especially the numerical experiments examining the impact of
413 temperature, [CO₂], nitrogen fertilization, and irrigation revealed some interesting features of the
414 spring wheat agroecosystem in India. All the fluxes have a similar pattern of high rise from 1980s
415 to 1990s, a small increase from 1990s to 2000s, and then a steep rise between 2000s and 2010s
416 (Figure 4:(b)). Although [CO₂] and Nitrogen fertilization increased at a constant rate throughout
417 the study period, the temperature and irrigation varied in an irregular manner. Higher temperatures
418 during the 2000s limited the rise in fluxes during this decade, and the lower water availability
419 during the 2010s caused a large spread in carbon fluxes in 2010s. The impact of [CO₂] measured
420 through the difference between S_{CON} and S_{CO₂} emphasised that with higher [CO₂] the carbon taken
421 up for photosynthesis increases and the overall ecosystem exchange from the croplands was higher
422 than the limited [CO₂] case. During the 2000s, a sudden dip in fluxes (Figure 4:(a)) was observed
423 that coincides with the higher temperature anomaly (Figure 5:(a)). However, the impact of added
424 water during this decade damped the negative effect of higher temperatures, which was evident
425 from the large spread seen in positive impact during this decade (Figure 6:(a-d)). Thus, the study
426 suggests that providing sufficient fertilizers and water through irrigation may be able to counteract
427 the adverse effects of high temperatures.

428 The simulated carbon fluxes are comparable to published values. The cumulative GPP and NEP
429 for the wheat-growing season observed at the Saharanpur site are 621 gC/m² and 192 gC/m² (Patel
430 et al., 2021). The GPP and NEP values simulated at the IARI site are 729.9 gC/m² and 523.3
431 gC/m². Although the GPP is comparable with Patel et al. (2021), NEP values simulated by ISAM
432 are not in the same range. The smaller NEP in Patel et al. (2021) is perhaps because the wheat crop
433 is grown immediately after sugarcane harvest with a fallow period of 30 days.

434 Additional work is required to overcome some of the limitations of this study. Perhaps the biggest
435 limitation of this study was in model evaluation. Ideally, multi-year data from numerous stations
436 across the study domain should be used for evaluation. However, carbon flux observations from
437 cropland in India were not available in the public domain. We used data from three agricultural

438 experimental sites in north India to evaluate the carbon fluxes simulated by ISAM. Even though
439 the model evaluation was sub-optimal, this study is a step in the right direction because this is the
440 first study to evaluate all terrestrial carbon fluxes simulated by a process-based model using site-
441 scale observations.

442 Second, we estimated the effect of water availability on carbon fluxes by comparing the control
443 simulation S_{CON} , where the crops do not experience any water stress, with the S_{Water} simulation,
444 where no irrigation is applied. The best way to understand the effect of irrigation would be to
445 conduct simulations driven by actual irrigation data. For this purpose, we need a gridded irrigation
446 time-series dataset. Unfortunately, such data does not exist (Gahlot et al., 2020) or is unrealistic in
447 magnitude and timing (Mathur and AchutaRao, 2020).

448 Finally, our simulations were conducted with a land model driven by externally imposed forcings.
449 In this approach, we ignored the feedback between the land surface and the atmosphere that can
450 be important, especially for the natural drivers like $[CO_2]$ and temperature. The next step moving
451 ahead would be to use a coupled land-atmosphere model that includes the feedback between the
452 terrestrial and atmospheric components of the carbon cycle.

453 **5 Conclusions**

454 We used the ISAM model equipped with a spring wheat module to study the carbon fluxes in
455 spring wheat agroecosystems across the wheat-growing regions of India for the last four decades.
456 The main conclusions from this study are as follows:

- 457 • The ISAM spring wheat module $ISAM_{dyn_wheat}$ was able to simulate the temporal patterns
458 of GPP, TER, and NEP at the site scale for the IARI experimental wheat farm. The
459 $ISAM_{dyn_wheat}$ model performed better compared to the generic $ISAM_{C3_crop}$ module.
- 460 • Carbon fluxes in spring wheat agro-ecosystems varied widely across the country due to
461 divergent climatic conditions and management practices, primarily due to difference in
462 planting dates. While central and eastern parts of the spring wheat-growing regions showed
463 high carbon fluxes during January, the northern parts exhibited their maximum carbon flux
464 values during March.
- 465 • The effects of increasing $[CO_2]$, nitrogen fertilization, and irrigation led to positive trends
466 in carbon fluxes in the last four decades. Nitrogen fertilization had the strongest effects,

467 followed by [CO₂] and then water availability. Providing sufficient fertilizers and water
468 through irrigation can counteract the adverse effects of high temperatures.

469 Understanding the variability in terrestrial carbon fluxes is essential for understanding the carbon
470 cycle. Agroecosystems cover large parts of the terrestrial biosphere, with the spring wheat
471 agroecosystem being one of India's largest land use types. This paper is one of the first long-term
472 regional-scale studies to look at carbon dynamics in an Indian agroecosystem. The model
473 developed in this study, after appropriate calibration, can be used to study other agroecosystems
474 as well. Very importantly, it can serve as a tool to conduct numerical experiments to study future
475 scenarios and the effects of external drivers. Thus, this study is likely to play a crucial role in
476 advancing our understanding of terrestrial carbon dynamics and our ability to simulate its
477 behaviour.

478 **Acknowledgments**

479 This work was partially supported by the Indian Space Research Organization (ISRO) Biosphere
480 Geosphere Program (IGBP).

481 **Open Research**

482 The site-scale observations measured at IARI, New Delhi and the ISAM simulated carbon fluxes
483 data are available at: <https://doi.org/10.5281/zenodo.5833742>

484 **References**

- 485 Baldocchi, D., Chu, H., and Reichstein, M. (2018). Inter-annual variability of net and gross
486 ecosystem carbon fluxes: A review. *Agricultural and Forest Meteorology*, 249, 520–533.
487 <https://doi.org/10.1016/J.AGRFORMET.2017.05.015>
- 488 Banger, K., Tian, H., Tao, B., Ren, W., Pan, S., Dangal, S., and Yang, J. (2015). Terrestrial net
489 primary productivity in India during 1901–2010: Contributions from multiple
490 environmental changes. *Climatic Change*, 132(4), 575–588. [https://doi.org/10.1007/s10584-](https://doi.org/10.1007/s10584-015-1448-5)
491 [015-1448-5](https://doi.org/10.1007/s10584-015-1448-5)
- 492 Bhatia, A., Kumar, A., Jain, N., Sehgal, V. K., and Pathak, H. (2014). Seasonal Variation in Net
493 Carbon-dioxide Exchange in Rice and Wheat Fields of Northern India. Asiaflux Workshop:
494 Bridging Atmospheric Flux Monitoring to National and International Climate Change
495 Initiatives, Proceedings Vol 1 18-23, August 2014, International Rice Research Institute
496 (IRRI), Los Banos, Philippines.
- 497 Chakraborty, S., Tiwari, Y. K., Deb Burman, P. K., Baidya Roy, S., and Valsala, V. (2020).
498 Observations and Modeling of GHG Concentrations and Fluxes Over India in *Assessment of*
499 *Climate Change over the Indian Region*, 73-92, Eds. R. Krishnan, et al., Springer Nature,

- 500 Singapore.
- 501 Chen, C., Li, D., Zhiqiu, G., Tang, J., Guo, X., Wang, L., et al. (2015) Seasonal and interannual
502 variations of carbon exchange over a rice-wheat rotation system on the North China Plain.
503 *Adv Atmos Sci*, 32, 1365–1380. <https://doi.org/10.1007/s00376-015-4253-1>
- 504 Chuine, I., and Régnière, J. (2017). Process-Based Models of Phenology for Plants and Animals.
505 *Annual Review of Ecology, Evolution, and Systematics*, 48(1), 159–182.
506 <https://doi.org/10.1146/annurev-ecolsys-110316-022706>
- 507 De Gonçalves, L. G. G., Borak, J. S., Costa, M. H., Saleska, S. R., Baker, I., Restrepo-Coupe, et
508 al. (2013). Overview of the large-scale biosphere-atmosphere experiment in amazonia data
509 model intercomparison project (LBA-DMIP). *Agricultural and Forest Meteorology*, 182–
510 183, 111–127. <https://doi.org/10.1016/j.agrformet.2013.04.030>
- 511 De Kauwe, M. G., Medlyn, B. E., Zaehle, S., Walker, A. P., Dietze, M. C., Hickler, T., et al.
512 (2013). Forest water use and water use efficiency at elevated CO₂ : a model-data
513 intercomparison at two contrasting temperate forest FACE sites. *Global Change Biology*,
514 19(6), 1759–1779. <https://doi.org/10.1111/gcb.12164>
- 515 Dentener, F. J. (2006). *Global Maps of Atmospheric Nitrogen Deposition, 1860, 1993, and 2050*.
516 <https://doi.org/10.3334/ORNLDAAC/830>
- 517 FAOSTAT. (2019). Food and Agriculture Organization of the United Nations, Rome, Italy.
518 Retrieved 14 May, 2021, from 2019 website: <http://www.fao.org/faostat/en/#data/QC>
- 519 Gahlot, S., Lin, T. S., Jain, A. K., Baidya Roy, S., Sehgal, V. K., and Dhakar, R. (2020). Impact
520 of environmental changes and land management practices on wheat production in India.
521 *Earth System Dynamics*, 11(3), 641–652. <https://doi.org/10.5194/esd-11-641-2020>
- 522 Gahlot, S., Shu, S., Jain, A. K., and Baidya Roy, S. (2017). Estimating Trends and Variation of
523 Net Biome Productivity in India for 1980–2012 Using a Land Surface Model. *Geophysical*
524 *Research Letters*, 44(22), 11,573-11,579. <https://doi.org/10.1002/2017GL075777>
- 525 Green, J. K., Seneviratne, S. I., Berg, A. M., Findell, K. L., Hagemann, S., Lawrence, D. M., et
526 al. (2019) Large influence of soil moisture on long-term terrestrial carbon
527 uptake. *Nature*, 565, 476–479. <https://doi.org/10.1038/s41586-018-0848-x>
- 528 Hatfield, J. L., and Prueger, J. H. (2015). Temperature extremes: Effect on plant growth and
529 development. *Weather and Climate Extremes*, 10, 4–10.
530 <https://doi.org/10.1016/j.wace.2015.08.001>
- 531 Huntzinger, D. N. N., Post, W. M. M., Wei, Y., Michalak, A. M. M., West, T. O. O., Jacobson,
532 A. R. R., et al. (2012). North American Carbon Program (NACP) regional interim
533 synthesis: Terrestrial biospheric model intercomparison. *Ecological Modelling*, 232, 144–
534 157. <https://doi.org/10.1016/j.ecolmodel.2012.02.004>
- 535 Hurtt, G. C., Chini, L. P., Frohling, S., Betts, R. A., Feddema, J., Fischer, G., et al. (2011).
536 Harmonization of land-use scenarios for the period 1500-2100: 600 years of global gridded
537 annual land-use transitions, wood harvest, and resulting secondary lands. *Climatic Change*,
538 109(1), 117–161. <https://doi.org/10.1007/S10584-011-0153-2/FIGURES/15>
- 539 Jain, A. K., and Yang, X. (2005). Modeling the effects of two different land cover change data
540 sets on the carbon stocks of plants and soils in concert with CO₂ and climate change.
541 *Global Biogeochemical Cycles*, 19(2), 20. <https://doi.org/10.1029/2004GB002349>
- 542 Jain, A., Yang, X., Kheshgi, H., McGuire, A. D., Post, W., and Kicklighter, D. (2009). Nitrogen
543 attenuation of terrestrial carbon cycle response to global environmental factors. *Global*
544 *Biogeochemical Cycles*, 23(4). <https://doi.org/10.1029/2009GB003519>
- 545 Jha, C. S., Thumaty, K. C., Rodda, S. R., Sonakia, A., and Dadhwal, V. K. (2013). Analysis of

- 546 carbon dioxide, water vapour and energy fluxes over an Indian teak mixed deciduous forest
547 for winter and summer months using eddy covariance technique. *Journal of Earth System*
548 *Science*, 122(5), 1259–1268. <https://doi.org/10.1007/s12040-013-0350-7>
- 549 Jones, J. W., Antle, J. M., Basso, B., Boote, K. J., Conant, R. T., Foster, I., et al. (2017). Brief
550 history of agricultural systems modeling. *Agricultural Systems*, 155, 240–254.
551 <https://doi.org/10.1016/j.agry.2016.05.014>
- 552 Koehler, A. K., Challinor, A. J., Hawkins, E., and Asseng, S. (2013). Influences of increasing
553 temperature on Indian wheat: quantifying limits to predictability. *Environmental Research*
554 *Letters*, 8(3), 034016. <https://doi.org/10.1088/1748-9326/8/3/034016>
- 555 Kumar, A., Bhatia, A., Sehgal, V.K., Tomer, R., Jain, N., and Pathak, H. (2021). Net Ecosystem
556 Exchange of Carbon Dioxide in Rice-Spring Wheat System of Northwestern Indo-Gangetic
557 Plains. *Land*, 10(7): 701. <https://doi.org/10.3390/land10070701>
- 558 Le Quéré, C., Andrew, R., Friedlingstein, P., Sitch, S., Hauck, J., Pongratz, J., et al. (2018).
559 Global Carbon Budget 2018. *Earth System Science Data*, 10(4), 2141–2194.
560 <https://doi.org/10.5194/essd-10-2141-2018>
- 561 Lin, T., Song, Y., Lawrence, P., Kheshgi, H. S., and Jain, A. K. (2021). Worldwide Maize and
562 Soybean Yield Response to Environmental and Management Factors Over the 20th and 21st
563 Centuries. *Journal of Geophysical Research: Biogeosciences*, 126(11).
564 <https://doi.org/10.1029/2021JG006304>
- 565 Lokupitiya, E., Denning, A. S., Schaefer, K., Ricciuto, D., Anderson, R., Arain, M. A., et al.
566 (2016). Carbon and energy fluxes in cropland ecosystems: a model-data comparison.
567 *Biogeochemistry*, 129(1–2), 53–76. <https://doi.org/10.1007/s10533-016-0219-3>
- 568 Luo, Y., Hui, D., and Zhang, D. (2006). Elevated CO₂ stimulates net accumulations of carbon
569 and nitrogen in land ecosystems: a meta-analysis. *Ecology*, 87(1), 53–63.
570 <https://doi.org/10.1890/04-1724>
- 571 MAFW (2017) Directorate of Economics and Statistics, Ministry of Agriculture, Govt. of India.
572 *Agricultural Statistics at a Glance 2016*. Retrieved from
573 <https://eands.dacnet.nic.in/PDF/Glance-2016.pdf>
- 574 Mathur, R., and AchutaRao, K. (2020). A modelling exploration of the sensitivity of the India's
575 climate to irrigation. *Climate Dynamics*, 54(3–4), 1851–1872.
576 <https://doi.org/10.1007/S00382-019-05090-8>
- 577 MOA (2016) Status paper on wheat; Directorate of Wheat Development Ministry of Agriculture
578 Govt. of India 180 pp., available at: <https://www.nfsm.gov.in/StatusPaper/Wheat2016.pdf>
579 (last access: 14 May 2021)
- 580 Monfreda, C., Ramankutty, N., and Foley, J. A. (2008). Farming the planet: 2. Geographic
581 distribution of crop areas, yields, physiological types, and net primary production in the
582 year 2000. *Global Biogeochemical Cycles*, 22(1), 1022.
583 <https://doi.org/10.1029/2007GB002947>
- 584 Mueller, N. D., Gerber, J. S., Johnston, M., Ray, D. K., Ramankutty, N., and Foley, J. A. (2012).
585 Closing yield gaps through nutrient and water management. *Nature*, 490(7419), 254–257.
586 <https://doi.org/10.1038/nature11420>
- 587 Ortiz, R., Sayre, K. D., Govaerts, B., Gupta, R., Subbarao, G. V., Ban, T., et al. (2008). Climate
588 change: Can wheat beat the heat? *Agriculture, Ecosystems and Environment*, 126(1–2), 46–
589 58. <https://doi.org/10.1016/j.agee.2008.01.019>
- 590 Patel, N. R., Dadhwal, V. K. and Saha, S. K. Measurement and Scaling of Carbon Dioxide (CO₂)
591 Exchanges in Wheat Using Flux-Tower and Remote Sensing. *J Indian Soc Remote Sens* 39,

- 592 383 (2011). <https://doi.org/10.1007/s12524-011-0107-1>
- 593 Patel, N. R., Pokhariyal, S., Chauhan, P. and Dadhwal, V.K. (2021). Dynamics of CO₂ fluxes and
594 controlling environmental factors in sugarcane (C₄)–wheat (C₃) ecosystem of dry sub-
595 humid region in India. *International Journal of Biometeorology*, 65, 1069–1084.
596 <https://doi.org/10.1007/s00484-021-02088-y>
- 597 Pillai, N. D., Nandy, S., Patel, N. R., Srinet, R., Watham, T., and Chauhan, P. (2019). Integration
598 of eddy covariance and process-based model for the intra-annual variability of carbon fluxes
599 in an Indian tropical forest. *Biodiversity and Conservation*, 28(8–9), 2123–2141.
600 <https://doi.org/10.1007/s10531-019-01770-3>
- 601 Ramadas, S., Kiran Kumar, T. M., and Pratap Singh, G. (2020). Wheat Production in India:
602 Trends and Prospects. In *Recent Advances in Grain Crops Research*.
603 <https://doi.org/10.5772/intechopen.86341>
- 604 Ren, X., Weitzel, M., O'Neill, B. C., Lawrence, P., Meiyappan, P., Levis, S., et al. (2018).
605 Avoided economic impacts of climate change on agriculture: integrating a land surface
606 model (CLM) with a global economic model (iPETS). *Climatic Change*, 146(3–4), 517–
607 531. <https://doi.org/10.1007/s10584-016-1791-1>
- 608 Reville, A., Emmel, C., D'Odorico, P., Buchmann, N., Hörtnagl, L., and Eugster, W. (2019).
609 Estimating cropland carbon fluxes: A process-based model evaluation at a Swiss crop-
610 rotation site. *Field Crops Research*, 234(January), 95–106.
611 <https://doi.org/10.1016/j.fcr.2019.02.006>
- 612 Saha, S., Das, B., Chatterjee, D., Sehgal, V. K., Chakraborty, D., and Pal, M. (2020). Crop
613 growth responses towards elevated atmospheric CO₂. In M. Hasanuzzaman (ed.), *Plant
614 Ecophysiology and Adaptation under Climate Change: Mechanisms and Perspectives I*, pp
615 147 - 198, Springer Nature, Singapore. https://doi.org/10.1007/978-981-15-2156-0_6
- 616 Sándor, R., Ehrhardt, F., Grace, P., Recous, S., Smith, P., Snow, V., et al. (2020). Ensemble
617 modelling of carbon fluxes in grasslands and croplands. *Field Crops Research*, 252(March).
618 <https://doi.org/10.1016/j.fcr.2020.107791>
- 619 Schmid, H. P. (1994). Source areas for scalars and scalar fluxes. *Boundary-Layer Meteorology*,
620 67(3), 293–318. <https://doi.org/10.1007/BF00713146>
- 621 Song, Y., Jain, A. K., and McIsaac, G. F. (2013). Implementation of dynamic crop growth
622 processes into a land surface model: Evaluation of energy, water and carbon fluxes under
623 corn and soybean rotation. *Biogeosciences*, 10(12), 8039–8066. <https://doi.org/10.5194/bg-10-8039-2013>
- 624
- 625 Sonkar, G., Mall, R. K., Banerjee, T., Singh, N., Kumar, T. V. L., and Chand, R. (2019).
626 Vulnerability of Indian wheat against rising temperature and aerosols. *Environmental
627 Pollution*, 254, 112946. <https://doi.org/10.1016/j.envpol.2019.07.114>
- 628 Viovy, N. (2018). *CRUNCEP Version 7 - Atmospheric Forcing Data for the Community Land
629 Model*. <https://doi.org/10.5065/PZ8F-F017>
- 630 Willmott, C. J., Robeson, S. M., and Matsuura, K. (2012). A refined index of model
631 performance. *International Journal of Climatology*, 32(13), 2088–2094.
632 <https://doi.org/10.1002/JOC.2419>
- 633 Yang, X., Wittig, V., Jain, A. K., and Post, W. (2009). Integration of nitrogen cycle dynamics
634 into the Integrated Science Assessment Model for the study of terrestrial ecosystem
635 responses to global change. *Global Biogeochemical Cycles*, 23(4), n/a-n/a.
636 <https://doi.org/10.1029/2009GB003474>
- 637 Yoshimoto, M., Oue, H., and Kobayashi, K. (2005). Energy balance and water use efficiency of

- 638 rice canopies under free-air CO₂ enrichment. *Agricultural and Forest Meteorology*, 133(1–
639 4), 226–246. <https://doi.org/10.1016/j.agrformet.2005.09.010>
- 640 Zeng, J., Matsunaga, T., Tan, Z. H., Saigusa, N., Shirai, T., Tang, Y., et al. (2020). Global
641 terrestrial carbon fluxes of 1999–2019 estimated by upscaling eddy covariance data with a
642 random forest. *Scientific Data* 2020 7:1, 7(1), 1–11. [https://doi.org/10.1038/s41597-020-](https://doi.org/10.1038/s41597-020-00653-5)
643 00653-5
- 644 Zhao, F., Zeng, N., Asrar, G., Friedlingstein, P., Ito, A., Jain, A., et al. (2016). Role of CO₂,
645 climate and land use in regulating the seasonal amplitude increase of carbon fluxes in
646 terrestrial ecosystems: A multimodel analysis. *Biogeosciences*, 13(17), 5121–5137.
647 <https://doi.org/10.5194/bg-13-5121-2016>
648